CHEMBIOCHEM

DOI: 10.1002/cbic.200800330

Plasmodium Telomeric Sequences: Structure, Stability and Quadruplex Targeting by Small Compounds

Anne De Cian,[a, b, c] Philippe Grellier,[d] Elisabeth Mouray,[d] Delphine Depoix,[d] Hélène Bertrand,[e] David Monchaud,[e] Marie-Paule Teulade-Fichou,[e] Jean-Louis Mergny,*[a, b, c] and Patrizia Alberti*[a, b, c]

The increasing resistance of Plasmodium falciparum *to the most commonly used antimalarial drugs makes it necessary to identify new therapeutic targets. The telomeres of the parasite could constitute an attractive target. They are composed of repetitions of a degenerate motif ($^{5'}$GGGTTYA$^{3'}$, where Y is T or C), different from the human one ($^{5'}$GGGTTA$^{3'}$). In this report we investigate the possibility of targeting* Plasmodium *telomeres with G-quadruplex ligands. Through solution hybridisation assays we provide evidence of the existence of a telomeric 3′ G-overhang in* P. falciparum *genomic DNA. Through UV spectroscopy studies we demonstrate that stable G-quadruplex structures are formed at physiological temperature by sequences composed of the degenerate* Plasmodium *telomeric motif. Through a FRET melting assay we show stabilisation of* Plasmodium *telomeric G-quadruplexes by a variety of ligands. Many of the tested ligands display strong quadruplex versus duplex selectivity, but show little discrimination between human and* Plasmodium *telomeric quadruplexes.*

Introduction

Telomeres are specialised nucleoprotein complexes that cap and protect the extremities of eukaryote chromosomes. In most eukaryotes, the telomeric DNA strand running from 5′ to 3′ consists of tandem repeats of a short motif that bears consecutive guanines.[1,2] This strand extends beyond the complementary strand and results in a single-stranded, G-rich 3′ overhang. Telomeric 3′ G-overhangs have been detected in a variety of organisms, including ciliates,[3,4] vertebrates,[5–7] yeasts[8] and plants,[9] and appear to be a conserved feature of eukaryotic telomeres.[10]

The inability of DNA polymerases to replicate linear chromosomes completely results in telomere shortening at each DNA replication. Telomere erosion can be compensated by a telomerase—a specialised reverse transcriptase, first identified in ciliates,[11] capable of adding telomeric repeats to the 3′ ends of telomeres. In humans, the 150–250 nucleotide-long 3′ G-overhang[5–7] is involved in the formation of a capping structure.[12] Its sequence ($^{5'}$GGGTTA$^{3'}$ repeats) makes it prone to folding into stable G-quadruplexes (Figure 1) under physiological conditions.[13] G-quadruplex stabilisation was shown to inhibit telomerase elongation in vitro,[14] and G-quadruplex-stabilising ligands were therefore initially considered as potential telomerase inhibitors.[15] Besides affecting telomere length, G-quadruplex ligands were also shown to induce short-term responses in human cells as a result of their ability to disrupt telomere structure (for a recent review, see ref. [16]). So far, G-quadruplex ligands have been investigated as potential inhibitors of cancer cell proliferation. Here, we investigate the possibility of targeting *Plasmodium falciparum* telomeres with G-quadruplex ligands as a potential strategy to interfere with human protozoan parasite infections.

P. falciparum is the protozoan parasite that causes the most severe form of human malaria. The parasite, which is transmitted by the bite of an infected *Anopheles* female mosquito, enters the bloodstream and invades hepatocytes. In hepatocytes it reproduces asexually and produces thousands of merozoites from a single parasite. Hepatocytic merozoites are released into the bloodstream and initiate the 48 h asexual intraerythrocytic cycle, in which several mitotic divisions occur, and produce 16–32 new merozoites. At the end of a cycle, the infected red blood cell bursts, and the released parasites invade other blood cells. *P. falciparum* resistance to the most commonly used antimalarial drugs makes it necessary to identify new therapeutic targets and drugs.[17] The 23 Mb haploid nu-

[a] *Dr. A. De Cian, Dr. J.-L. Mergny, Dr. P. Alberti*
INSERM, U565, Paris Cedex 05, 75231 (France)
Fax: (+33) 1-40-79-37-05
E-mail: mergny@mnhn.fr
alberti@mnhn.fr

[b] *Dr. A. De Cian, Dr. J.-L. Mergny, Dr. P. Alberti*
CNRS, UMR5153, Paris Cedex 05, 75231 (France)

[c] *Dr. A. De Cian, Dr. J.-L. Mergny, Dr. P. Alberti*
Muséum National d'Histoire Naturelle, USM 503
Régulation et Dynamique des Génomes
43 Rue Cuvier, CP26, Paris Cedex 05, 75231 (France)

[d] *Prof. P. Grellier, Dr. E. Mouray, Dr. D. Depoix*
Muséum National d'Histoire Naturelle, USM 504-EA3335
Biologie Fonctionnelle des Protozoaires
61 Rue Buffon, CP52, Paris Cedex 05, 75231 (France)

[e] *H. Bertrand, Dr. D. Monchaud, Dr. M.-P. Teulade-Fichou*
Institut Curie, Section Recherche, CNRS UMR 176
Centre Universitaire Paris XI
Bâtiment 110, 91405 Orsay (France)

Supporting information for this article is available on the WWW under http://www.chembiochem.org or from the author.

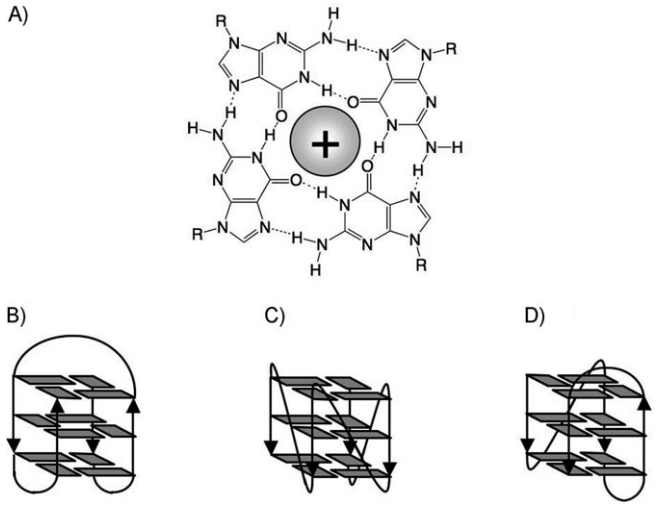

Figure 1. A) G-quadruplexes are four-stranded structures based on the formation and stacking of quartets of coplanar guanines or G-quartets. These structures are stabilised by several cations, in particular K^+ and Na^+. B), C), and D) Schematic representations of resolved structures of the human telomeric sequence, as examples of intramolecular folding: B) antiparallel folding based on the NMR structure in Na^+,[43] C) parallel folding based on the X-ray structure in K^+,[55] and D) hybrid-type folding based on the NMR structure in K^+ [44,45] (a second hybrid-type quadruplex, not shown, had been resolved in K^+ [57,58]).

clear genome of *P. falciparum*, which is organised into 14 chromosomes, is extremely AT rich (>80%).[18] Its telomeres have a 1.3 kb mean length[19] and are composed of a degenerate motif, with ^{5}'GGGTTYA^3' (where Y is T or C) being the most abundant (≈80%).[20] This repeat appears to be common to all *Plasmodium* species.[21] *P. falciparum* telomeres also appear to play a role in the regulation of subtelomeric gene families that encode important virulence factors.[22,23] Telomerase activity has been detected during the *P. falciparum* erythrocytic stage and in gametocytes,[20,24] and we have detected telomerase activity in other *Plasmodium* species (the rodent parasites *P. yoelii yoelii* and *P. berghei*; P.A., D.D., unpublished results). The putative genes for the catalytic subunit of telomerase and its RNA component were recently identified.[25,26]

In order to investigate the possibility of targeting *Plasmodium* telomeres with G-quadruplex ligands, we addressed the following questions:

1) Do *P. falciparum* telomeres end with a 3′ G-overhang?
2) Can the degenerate motif of the *Plasmodium* telomeric G-strand fold into stable G-quadruplex structures?
3) Is it possible to stabilise these structures with small synthetic or natural compounds?
4) Finally, can a ligand discriminate between quadruplexes at the telomeres of the parasite and quadruplexes at the telomeres of its human host?

To answer these questions, we first carried out solution hybridisation assays in order to detect telomeric 3′ G-overhang in *P. falciparum* genomic DNA. We then undertook a UV spectroscopic investigation of the eight possible sequences consisting of 3.5 repetitions of the *Plasmodium* degenerate telomeric motif ^{5}'GGGTTYA^3' (sequences Pf1 to Pf8 reported in Table 1). Using a competitive FRET melting assay, we then studied the interaction of several known G-quadruplex ligands with the *Plasmodium* telomeric sequences. Different families of compounds—quinacridine derivatives,[27,28] neomycin-capped macrocyclic compounds,[29] bisquinolinium compounds,[30] a copper–terpyridine complex[31] and an ethidium derivative (Figure 2)—were tested.[32,33] Four well studied G-quadruplex ligands—the cationic porphyrin TMPyP4,[34] the perylene derivative PIPER,[35] the trisubstituted acridine BRACO-19[36,37] and the natural compound telomestatin (Figure 2)—were also tested.[38,39]

Table 1. Oligonucleotide sequences and stability.

	Oligonucleotide sequences	T_m [°C]		ΔH° [kcal mol^{-1}]	ΔG° (37 °C) [kcal mol^{-1}]
		NaCl	KCl	NaCl[a]	NaCl[a]
Pf1	$^5G_3TTTAG_3TTTAG_3TTTAG_3^{3'}$	58	65	−59	−3.6
Pf2	$^5G_3TTTAG_3TTTAG_3TTCAG_3^{3'}$	54	63	−50	−2.5
Pf3	$^5G_3TTTAG_3TTCAG_3TTTAG_3^{3'}$	55	64	−53	−2.8
Pf4	$^5G_3TTTAG_3TTCAG_3TTCAG_3^{3'}$	54	63	−50	−2.5
Pf5	$^5G_3TTCAG_3TTTAG_3TTTAG_3^{3'}$	54	64	−55	−2.9
Pf6	$^5G_3TTCAG_3TTTAG_3TTCAG_3^{3'}$	55	63	−55	−2.8
Pf7	$^5G_3TTCAG_3TTCAG_3TTTAG_3^{3'}$	55	64	−55	−2.9
Pf8	$^5G_3TTCAG_3TTCAG_3TTCAG_3^{3'}$	52	62	−48	−2.2
21G	$^5G_3TTAG_3TTAG_3TTAG_3^{3'}$	59	67	−54	−3.7

T_m (±1 °C) and ΔH° values (±10%) were determined by analysis of melting transitions (at 295 nm) of oligonucleotides (3 μM) in a cacodylic acid buffer (10 mM, pH 7.2, adjusted with LiOH) containing NaCl or KCl (100 mM). In LiCl (100 mM), the T_m values were around 27 °C; 21G is the human telomeric sequence. [a] ΔH° values were determined by linearly fitting ($R > 0.998$) a van't Hoff representation of the equilibrium constants determined by a two-state model, with the assumption of low- and high-temperature linear baseline corrections; ΔG° values were extrapolated at 37 °C. If the uncertainty in ΔH° determination (due to low- and high-temperature baseline determination) is taken into account, the differences between the Pf2–Pf7 thermodynamic parameters cannot be considered significant. The ΔH° and ΔG° values (37 °C) in KCl were around (−63 ± 5) and (−4.9 ± 0.6) kcal mol^{-1}, respectively; they are not listed, because they are affected by a greater degree of uncertainty than in NaCl, due to a greater uncertainty in high-temperature baseline determination and to ΔG° extrapolation at a temperature (37 °C) far below the range of temperatures at which melting transitions occur.

Results

Evidence for a 3′ G-overhang at *P. falciparum* telomeres

In order to determine whether the *P. falciparum* telomeres end with a 3′ G-overhang, solution hybridisation assays under non-denaturing conditions were carried out on the FCB1 *P. falciparum* strain (schizont stage).

In a first assay, genomic DNA was incubated at 37 °C or 50 °C with a radiolabelled probe complementary either to the telomeric G-rich strand (*C-probe: $d(TGAACCC)_3$, $^{32}PO_4$ at the 5′-end) or to the telomeric C-rich strand (*G-probe: $d(GGGTTTA)_3$, $^{32}PO_4$ at the 5′ end). After migration in an agarose gel, radioactivity detection revealed that in relation to the *G-probe, the

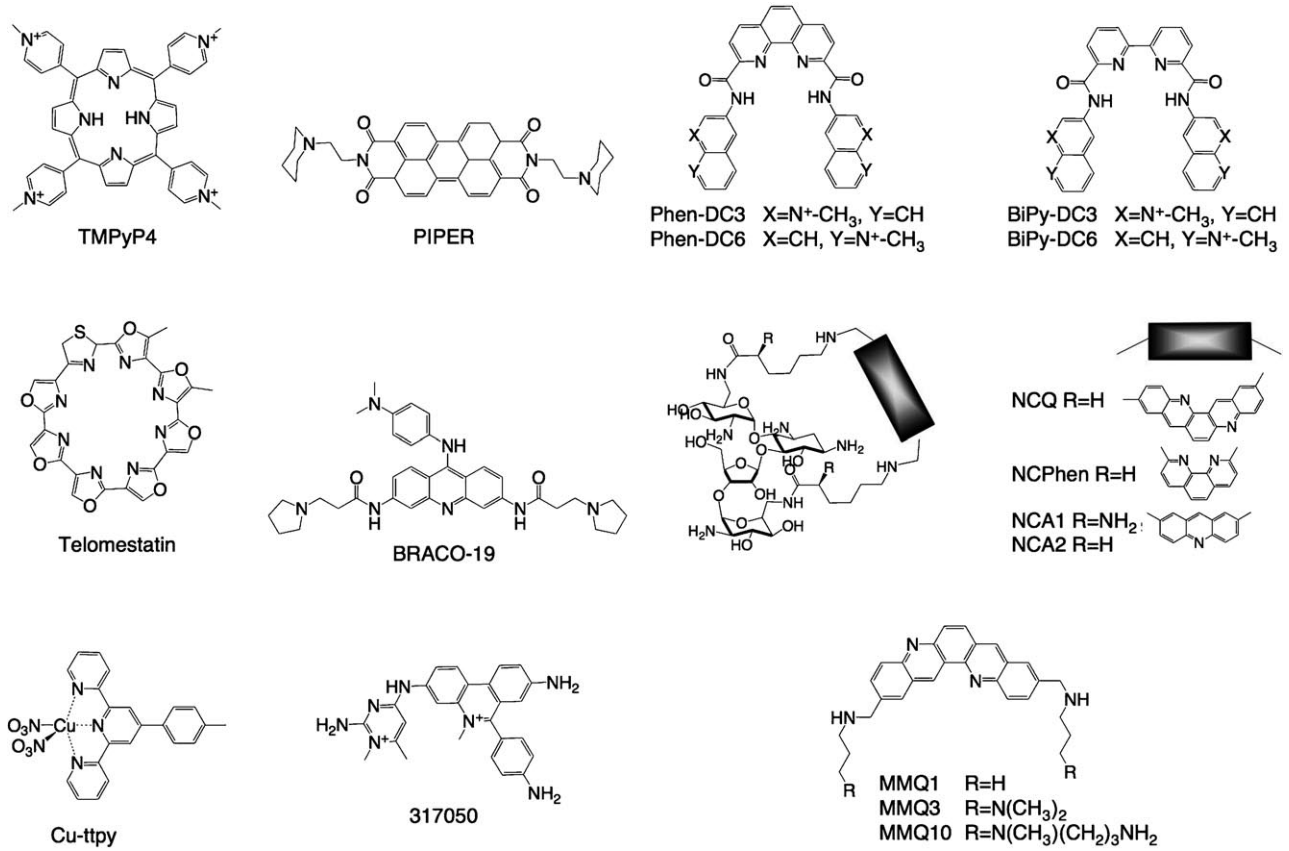

Figure 2. Formulae of the tested compounds. MMQs are mono-*meta*-quinacridine derivatives,[27,28] NCQ, NCPhen and NCAs are macrocyclic compounds composed of an aromatic unit (quinacridine, phenanthroline or acridine) capped with a neomycin moiety,[29] and Phen-DCs and BiPy-DCs are crescent-shaped bisquinolinium compounds with phenanthroline or bipyridine central units, respectively.[30]

*C-probe strongly hybridised to the genomic DNA (Figure 3A). The strong difference in C- and G-probe hybridisation signals could be ascribed neither to G-probe intermolecular assembly (Figure S1 in the Supporting Information) nor to folding of *Plasmodium* telomeric C-strand into i-motifs (using TDS and UV-melting experiments we verified that the sequence d-$(CCCTAAA)_3CCC$, which mimics the *Plasmodium* telomeric C-strand did not fold into an i-motif at the pH of the hybridisation experiments; data not shown).

In telomere restriction fragments (TRF) assays, genomic DNA was digested by four enzymes that do not cut *Plasmodium* telomeric sequences.[19] A Southern blot of the digested genomic DNA with the telomeric *C-probe (denaturing TRF assay) revealed a strong hybridisation signal to fragments of about 1–1.6 kb and also to longer fragments (approximately 3 kb; Figure 3B, right). This was consistent with what had been observed in other *P. falciparum* strains: 1.3 kb is the reported mean length of several *P. falciparum* strains, and a two-peak hybridisation pattern was previously observed in another strain.[19] A similar hybridisation pattern was observed in a native TRF assay upon incubation of the digested DNA with the *C-probe. Unlike the *C-probe, the *G-probe did not hybridise to telomeric fragments in the native TRF assay (Figure 3B, centre). These TRF assays support the existence of a G-overhang at *P. falciparum* telomeres.

Finally, in a telomeric–oligonucleotide ligation assay (T-OLA),[40] genomic DNA (treated or untreated with exonucleases) was incubated with the *C-probe. Consecutively hybridised probes were then ligated. The *C-probe hybridised to genomic DNA under nondenaturing conditions (Figure 3C, ^{32}P native gel), and long concatenated *C-probes (up to $\approx$200 nucleotides) were detected in a denaturing gel (Figure 3C, ^{32}P denaturing gel). Treatment of genomic DNA with exonucleases before incubation with the *C-probe verified that the detected signals arose from hybridisation to a 3′ overhang. Indeed, when genomic DNA was treated with exonuclease I, which degrades single-stranded DNA in the 3′ to 5′ direction, the hybridisation signals were strongly reduced; when treated with T7 exonuclease, which removes nucleotides from 5′ ends in double-stranded DNA, the hybridisation signals were strongly amplified (Figure 3C, ^{32}P native and denaturing gels). Similar hybridisation patterns were obtained with genomic DNA from parasites at the ring stage—a parasite stage in which DNA does not undergo replication (data not shown); this indicates that the observed hybridisation patterns were not due to the presence of incomplete strand synthesis at chromosome ends.

Taken together, the solution hybridisation assays strongly support the existence of a telomeric 3′ G-overhang in *P. falciparum* genomic DNA. The oligonucleotide ligation assay does not provide direct information about the length distribution of

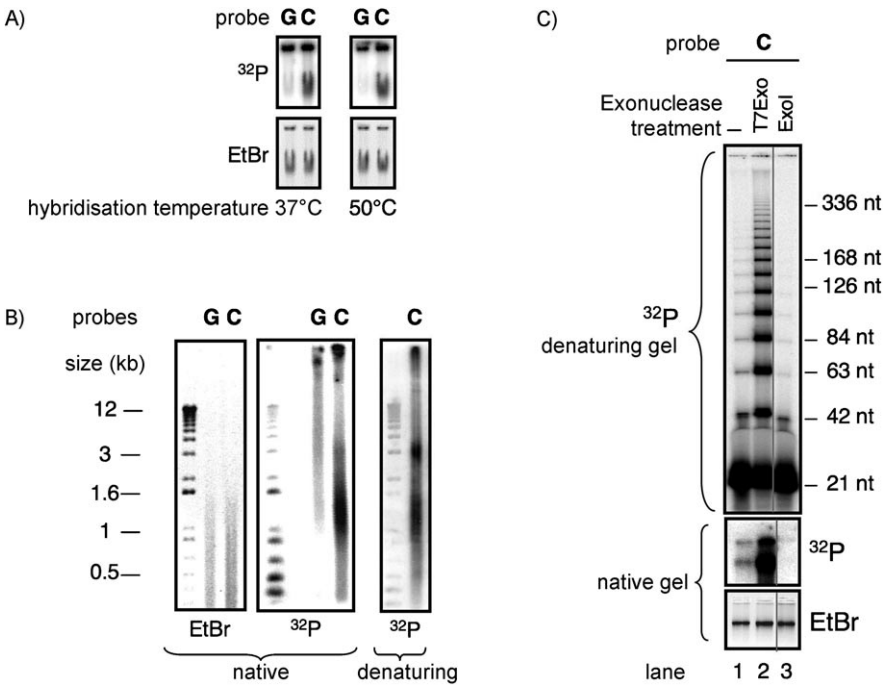

Figure 3. Solution hybridisation assays under nondenaturing conditions. A) Agarose gels of *P. falciparum* genomic DNA incubated with *G-probe ($d(GGGTTTA)_3$, radiolabelled at 5′ end) or *C-probe ($d(TGAACCC)_3$, radiolabelled at 5′ end) at 37 or 50 °C. Top panels: gels imaged by using ^{32}P radioactivity to detect probe hybridisation; lower panels: gels imaged by using ethidium bromide (EtBr) fluorescence as DNA loading control. B) Native and denaturing TRF assays. Left and central panels: agarose gel of *P. falciparum* telomere restriction fragments incubated with the *G- or *C-probe at 37 °C, imaged by using ^{32}P radioactivity to detect probe hybridisation (central panel) and by ethidium fluorescence as DNA loading control (left panel). Right panel: Southern blot of telomere restriction fragments with the *C-probe. C) T-OLA; native gel: agarose gel of samples of *P. falciparum* genomic DNA after incubation with the *C-probe and ligation of consecutively hybridised probes, imaged by using ^{32}P radioactivity and ethidium fluorescence. Denaturing gel: 5% denaturing polyacrylamide gel of the same samples, imaged by using ^{32}P radioactivity to detect ligated *C-probes. The assay was performed with genomic DNA either untreated (lane 1) or treated with T7 exonuclease or exonuclease I (lanes 2 and 3, respectively).

this overhang; nevertheless, it allowed the presence of relatively long overhangs that are capable, in principle, of folding into intramolecular G-quadruplexes, to be revealed.

G-quadruplex folding and stability of *Plasmodium* telomeric sequences

Having demonstrated the presence of a telomeric 3′ G-overhang at *P. falciparum* telomeres, we then investigated whether sequences mimicking this overhang form quadruplex structures. We undertook a UV spectroscopic investigation of the eight possible sequences that mimic 3.5 repetitions of the *Plasmodium* degenerate telomeric motif $^{5'}GGGTTYA^{3'}$, where Y is T or C (sequences Pf1 to Pf8, Table 1). These oligonucleotides each bear four runs of consecutive guanines, which is the minimum number required for the formation of an intramolecular G-quadruplex.

Thermal difference spectra: The thermal difference spectrum (TDS) of a nucleic acid in solution is defined as the difference between the absorbance spectrum at high temperature (unfolded form) and that at low temperature (folded form). The global shape of a TDS provides information about the structure adopted by a nucleic acid sequence.[41] The TDS signatures of the eight *Plasmodium* telomeric sequences (Pf1 to Pf8) were characteristic of G-quadruplex structures, with two positive peaks at around 240 and 270 nm, and a negative peak at 295 nm (Figure 4). The thermal difference spectra in NaCl (Figure 4A) differed slightly from those in KCl (Figure 4B) in the ratio between the peak at 240 nm and the peak at 273 nm (0.64 ± 0.09 and 0.93 ± 0.07, respectively). These differences in NaCl and KCl TDS profiles have been observed for many other G-quadruplex-forming sequences.[41,42]

Circular dichroism spectra: CD spectra were recorded at 20 °C. For all the studied sequences, the equilibria at this temperature were strongly shifted towards the folded forms, as shown by the thermal melting profiles (Figure 4C and D). The eight Pf sequences displayed different CD spectra in sodium and in potassium. In NaCl, the spectra each exhibited two positive bands near 245 and 295 nm and a negative band near 265 nm (Figure 4E). In KCl, the spectra each exhibited a positive band at 290 nm and a shoulder at lower wavelength (Figure 4F). These spectra were similar to those of the human telomeric sequence 21G. Two conclusions can be drawn from these CD signatures. 1) Consistent with the TDS spectra, the CD signatures displayed by the eight Pf sequences are characteristic of G-quadruplex structures, both in NaCl and in KCl.[43,44] 2) The difference between the NaCl and KCl signatures suggests a different folding topology[45] or a different equilibrium between multiple possible conformations according to the nature of the monocation present in solution.

UV melting experiments: Under our experimental conditions, the melting profiles (recorded at 245, 260, 273 and 295 nm) were reversible and presented single melting transitions both in sodium and in potassium (only Pf1, Pf8 and 21G transitions are shown in Figure 4C and D; all transitions are available in Figure S2). Melting temperature values were graphically determined[46] and are reported in Table 1. In the presence of a given monocation, the eight *Plasmodium* telomeric sequences displayed similar thermal stabilities: the mean values of their T_m values in LiCl, NaCl and KCl were 27 (± 1) °C, 55 (± 2) °C and 64 (± 1) °C, respectively (Table 1). This dependence of stability on the nature of the monocation is characteristic of G-quadruplex structures and is a further argument, along with the TDS

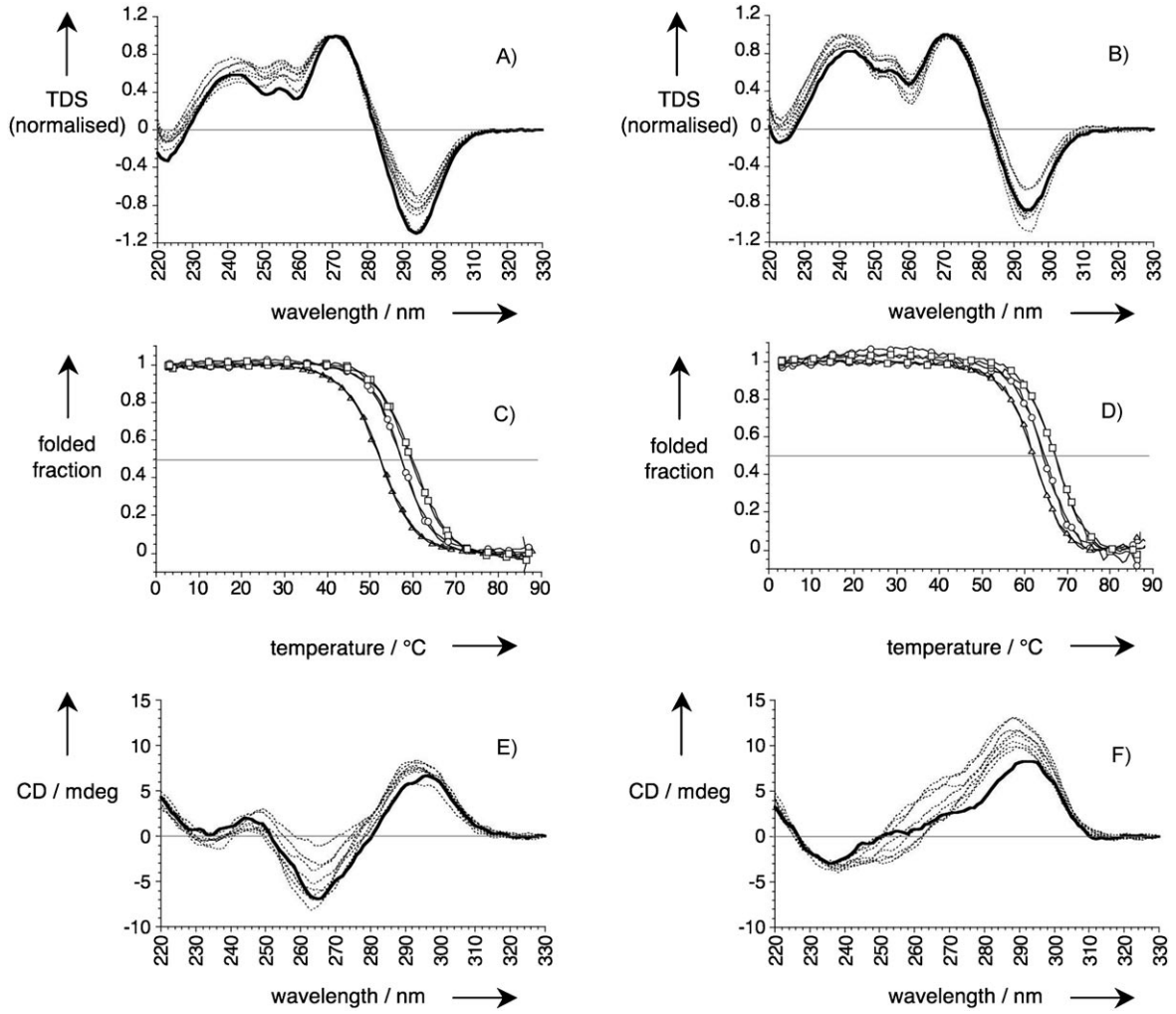

Figure 4. Spectroscopic analysis of the Pf sequences. Normalised thermal difference spectra of the eight *Plasmodium* telomeric sequences Pf1–Pf8 (····) and of the human telomeric sequence 21G (——) in A) NaCl and B) KCl. Oligonucleotide folded fraction as a function of temperature in C) NaCl and D) KCl for Pf1 (△), Pf8 (○) and 21G (□). The folded fractions were deduced from melting curves recorded at 295 nm, with the assumption of low- and high-temperature linear baseline corrections. Circular dichroism spectra of the eight *Plasmodium* telomeric sequences Pf1–Pf8 (····) and of the human telomeric sequence 21G (——) in E) NaCl and F) KCl at 20 °C. All the measurements were carried out with 3 μM oligonucleotide in a cacodylic acid buffer (10 mM, pH 7.2, adjusted with LiOH) containing NaCl or KCl (100 mM). A colour Figure reporting TDS, CD spectra and all melting profiles is available in Figure S2.

and CD signatures, in support of the formation of G-quadruplex structures by the eight *Plasmodium* telomeric sequences. The NaCl and KCl melting profiles and CD spectra did not change upon a tenfold increase in oligonucleotide concentration (30 μM, data not shown); this indicates intramolecular folding in this range of concentrations. The mean values of the T_m values of the eight Pf sequences were 4 and 3 °C lower in sodium and potassium, respectively, than those of the telomeric human sequence 21G. The sequence Pf1, which bears all TTTA loops, appeared to be the most stable with a T_m value that approached the T_m of the human sequence 21G, whereas the sequence Pf8, which bears all TTCA loops, was the least stable. A van't Hoff representation[46] of the melting curves, analysed by a two-state model, could be linearly fitted (with linear regression coefficients >0.998). In NaCl, the Gibbs free energy (ΔG°) extrapolated at 37 °C varied from -3.6 kcal mol^{-1} for Pf1 to -2.2 kcal mol^{-1} for Pf8. The other Pf sequences (from Pf2 to Pf7) were characterized by ΔG° values at 37 °C between -2.5 and -2.9 kcal mol^{-1} (Table 1). In KCl, the ΔH° values of the Pf and 21G sequences were around (-63 ± 5) kcal mol^{-1}, whereas the ΔG° values extrapolated at 37 °C were around (-4.9 ± 0.6) kcal mol^{-1}.

These experiments demonstrate that stable quadruplexes were formed at physiological temperatures by sequences containing the degenerate *Plasmodium* telomeric motif.

Interaction of known G-quadruplex ligands with *Plasmodium* telomeric G-quadruplexes and competition with duplex DNA

Having established that the *Plasmodium* G-rich telomeric sequences are prone to quadruplex formation, we next investigated whether these quadruplexes were recognised by G-quadruplex ligands known to interact with the human telomeric quadruplex. Using a FRET melting assay,[47] we studied the interaction of several known G-quadruplex ligands (Figure 2)

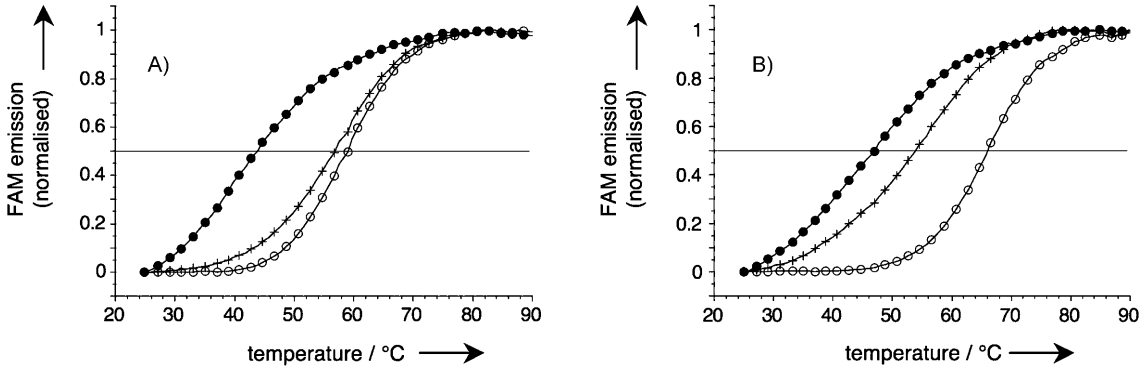

Figure 5. Examples of FRET melting experiments. A) FPf1T alone (●); FPf1T in the presence of NCA1 (○); FPf1T in the presence of NCA1 and of the duplex competitor ds26 (+). B) FPf8T alone (●); FPf8T in the presence of MMQ10 (○); FPf8T in the presence of MMQ10 and ds26 (+). The experiments were performed with double-labelled oligonucleotide (0.2 μM), ligand (1 μM) and ds26 (3 μM), in a cacodylic acid buffer (10 mM, pH 7.2, adjusted with LiOH) containing NaCl (100 mM).

with the *Plasmodium* telomeric sequences and compared the results with those obtained with the human telomeric sequence. Three double-labelled oligonucleotides (FPf1T, FPf8T and F21GT) were used; they corresponded to the *Plasmodium* Pf1 (all TTTA loops) and Pf8 (all TTCA loops) sequences and to the human 21G sequence coupled to a 6-carboxyfluorescein (FAM) and to a carboxytetramethylrhodamine (TAMRA). Upon G-quadruplex unfolding, the distance between the donor FAM and the acceptor TAMRA increased, which led to a decrease in FRET efficiency and, as a consequence, to an increase in FAM emission. Monitoring of the FAM emission as a function of temperature allows determination of the temperature of half-dissociation ($T_{1/2}$) as described in the Experimental Section. Figure 5A and B shows two examples of FRET melting experiments with FPf1T and FPf8T, respectively. The difference between the $T_{1/2}$ temperatures in the absence and in the presence of a given compound ($\Delta T_{1/2}$) provides a measure of the quadruplex thermal stabilisation induced by the compound (Figure 5). The quadruplex versus duplex selectivity of a compound was then investigated by addition of a duplex competitor (Figure 5; ds26). For each compound, the selectivity (S) was defined as the ratio between the $\Delta T_{1/2}$ values in the presence and in the absence of duplex competitor: $S = \Delta T_{1/2}$ (+ds26)/$\Delta T_{1/2}$(−ds26). For a given G-quadruplex and a given duplex competitor, S reflects the preferential binding of a compound to the quadruplex ($S \rightarrow 1$) or to the duplex ($S \rightarrow 0$). FRET melting experiments were carried out in the presence of both sodium and potassium (all data in NaCl and KCl are available in Figure S3). Here, we have chosen to report only the data in NaCl, since biphasic melting curves were observed in KCl in the presence of some ligands (as already reported[47]). For these ligands, $\Delta T_{1/2}$ values in KCl have to be considered with more caution. Quadruplex–ligand interaction can depend on quadruplex structure; we verified that the CD spectra of the three double-labelled quadruplexes FPf1T, FPf8T and F21GT were similar to those of Pf1, Pf8 and 21G, both in NaCl and in KCl; this suggests that their folding topologies were not altered by the two fluorescent reporters (data not shown).

Within the uncertainty of the experimental data, each compound stabilised the three telomeric quadruplexes to roughly the same extent, at the chosen concentration of 1 μM. This is easily seen by plotting the $\Delta T_{1/2}$ values induced on FPf1T or FPf8T versus the $\Delta T_{1/2}$ induced on F21GT (Figure 6A and B): all experimental points were close to the straight line (slope of about one) and, for the majority of compounds, the distance from this straight line was within the standard deviations (not shown). For all the tested compounds, the quadruplex versus duplex selectivity values obtained for the *Plasmodium* telomeric sequences were similar to those obtained for the human one (at 10 μM duplex competitor; Figure 6C). For all the three telomeric quadruplexes, the two bisquinolinium compounds Phen-DC3 and Phen-DC6 induced the strongest thermal stabilisation, followed by telomestatin, the porphyrin TMPyP4 and the quinacridine derivative MMQ10 ($\Delta T_{1/2} > 20\,^{\circ}C$). TMPyP4 and MMQ10 displayed poor selectivity ($S \approx 0$ and $S \approx 0.2$, respectively), whereas Phen-DC3, Phen-DC6 and telomestatin were among the most selective compounds ($S \approx 0.8$). Despite a lower thermal stabilisation capability, other compounds—the two bisquinolinium compounds BiPy-DC3 and BiPy-DC6 ($S \approx 0.8$), the two neomycin-capped acridines NCA1 and NCA2 ($S \approx 0.7$) and the copper–terpyridine complex Cu-ttpy ($S \approx 1$)—displayed strong selectivity. The stabilisation and selectivity profiles we obtained for the human telomeric sequence F21GT were consistent with those reported in the literature.[29–31]

Most of the ligands induced stronger quadruplex stabilisation ($\Delta T_{1/2}$) in KCl than in NaCl, and displayed stronger quadruplex versus duplex selectivity (Figure S3). Nevertheless, both in KCl and in NaCl, all the tested compounds displayed, within the limits of experimental error, the same stabilisation and selectivity profiles towards the three telomeric sequences.

From these data we conclude that *Plasmodium* telomeric quadruplexes are recognized by a variety of ligands and that many ligands exhibit a strong selectivity for quadruplex structures relative to a duplex structure, but show little discrimination between the human and *Plasmodium* sequences, either in NaCl or in KCl.

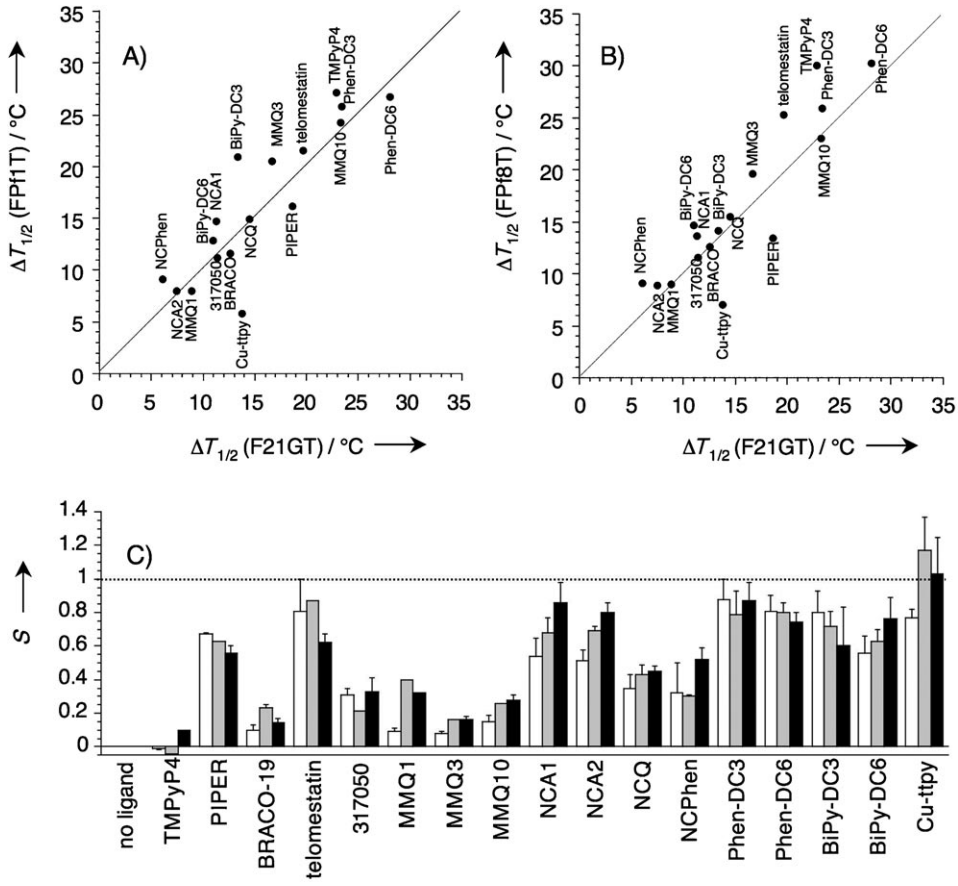

Figure 6. A), B) Thermal stabilisation ($\Delta T_{1/2}$) induced by the different compounds on the *Plasmodiu*m telomeric quadruplexes FPf1T and FPf8T versus $\Delta T_{1/2}$ induced on the human telomeric quadruplex F21GT (for clarity of representation, the error bars are reported only in the Supporting Information). C) Quadruplex versus duplex selectivity (S, the ratio between $\Delta T_{1/2}$ in the presence and absence of duplex competitor ds26: $S = \Delta T_{1/2}(+\text{ds26})/\Delta T_{1/2}(-\text{ds26})$) for F21GT (□), FPf1T (▣) and FPf8T (■). The experiments were carried out with doubly labelled oligonucleotide (0.2 μM), ligand (1 μM) and ds26 (10 μM), in a cacodylic acid buffer (10 mM, pH 7.2, adjusted with LiOH) containing NaCl (100 mM). Under these experimental conditions, the $T_{1/2}$ values of FPf1T, FPf8T and F21GT alone were 43.8, 44.7 and 49.7 °C (±1 °C), respectively; the duplex competitor ds26 had a T_m value of around 70 °C and did not affect the melting transitions of the three quadruplexes.

Discussion

Telomere protection and maintenance are essential for the proliferation of eukaryotic cells. Thus, use of drugs that impair telomeric functions in rapidly proliferating protozoan parasites might be a potential strategy to stop progress of the infection. In principle, stabilisation of G-quadruplex structures at telomeres might alter the telomere nucleoprotein structure by several mechanisms of action: by impairing correct processing of the 3′ G-overhang, by impairing refolding of telomeres in a capping structure, by perturbing interaction with telomere-associated proteins, or by interfering with telomere replication. Very little is known about telomere regulation in *P. falciparum*; its extremely AT-rich genome makes telomeres a very attractive target for G-quadruplex ligands. The aim of this study was to investigate the possibility of targeting *P. falciparum* telomeres with G-quadruplex ligands.

To this end, we first investigated the existence of a 3′ G-overhang at *P. falciparum* telomeres. In solution hybridisation assays under nondenaturing conditions, we detected hybridisation signals on *P. falciparum* genomic DNA that strongly supported the existence of such an overhang. Long hybridisation products were detected in a telomeric–oligonucleotide ligation assay; this suggests the presence of long 3′ G-overhangs. An in-depth investigation of the length distribution and dynamics of *P. falciparum* telomeric overhangs was beyond the scope of this study and is currently in progress.

We then investigated the structure and the stability of the eight sequences Pf1–Pf8, which correspond to all the possible sequences formed by about four repetitions of the *Plasmodium* degenerate telomeric motif $^{5'}$GGGTTYA$^{3'}$, using UV spectroscopy. Three lines of experimental evidence showed the formation of G-quadruplex structures by all the eight sequences: 1) the profiles of their thermal difference spectra, 2) their CD signatures, and 3) the dependence of their melting temperatures upon the nature of the monocation present in the solution ($T_m(K^+) > T_m(Na^+) > T_m(Li^+)$). All the Pf G-quadruplexes were stable at physiological temperature (37 °C), both in sodium and potassium solutions. Pf1 (all TTTA loops) appeared to be the most stable, whereas Pf8 (all TTCA loops) was the least stable. The T_m values of the Pf sequences were on average a few degrees lower than those of the human telomeric sequence 21G (TTA loops). The same trend was found when thermodynamic stability was analysed by a van't Hoff analysis. A decrease in stability with increasing loop length was reported for similar sequences bearing T_n loops.[48] The similarity of Pf and 21G CD signatures in the presence of a given monocation (sodium or potassium) makes it tempting to speculate that all the eight Pf sequences fold into structures similar to those resolved for the human telomeric sequence (antiparallel folding in NaCl and hybrid-type folding in KCl). Nevertheless, speculations about folding topology drawn from CD signatures must be considered with caution. The only relevant conclusion that can be drawn from Pf CD spectra is the following: as in the case of the human telomeric sequence 21G, the eight Pf sequences displayed different CD signatures in NaCl and KCl; this indicates different folding topologies or equilibria among multiple possible conformations according to the nature of the monocation present in

solution. Preliminary NMR spectroscopy studies on the Pf1 sequence revealed the presence of two major G-quadruplex structures in the presence of KCl (Anh Tuan Phan, personal communication). In nondenaturing PAGE experiments in sodium or potassium, the Pf sequences migrated as single bands with the same mobility, which was slightly slower than that of the 21G sequence (Figure S4). Hence, for a given monocation, no dramatic structural differences between the eight Pf sequences could be detected.[49]

We then used a competitive FRET melting assay to study the interactions of several known G-quadruplex ligands with the *Plasmodium* telomeric sequences. All the tested compounds displayed roughly the same stabilisation and quadruplex versus duplex selectivity profiles for the two *Plasmodium* telomeric sequences (FPf1T and FPf8T) and the human one (F21GT), both in sodium and in potassium. The stabilisation and selectivity profiles we obtained suggest that each of the tested compounds has roughly the same affinity for each of the three different quadruplexes. This means that the compounds we tested could not discriminate between *Plasmodium* and human telomeric quadruplexes, despite the differences in loop length and loop sequences. This result is not unexpected, since all the tested ligands present aromatic surfaces suitable for π–π interactions with a G-quartet surface; probably they stabilise G-quadruplex structures by stacking onto the terminal G-quartet(s). For an antimalarial approach based on targeting *P. falciparum* telomeres, discrimination between G-quadruplexes at parasite telomeres and G-quadruplexes at the telomeres of its human host should, in principle, reduce toxicity. Discrimination could be achievable through ligands that strongly interact with the "variable" structural features of G-quadruplexes, in particular with loops. High-resolution structural studies of the Pf sequences should be helpful for rational design of ligands capable of discriminating between the *Plasmodium* and the human telomeric G-quadruplexes. Nevertheless, ligand discrimination between human and *Plasmodium* telomeric quadruplexes (target selectivity) cannot be assumed, a priori, as a necessary condition for a therapeutic strategy. Very little is known about telomere regulation in *P. falciparum*; response or time-response to telomere perturbation might be different in parasite and in human cells. For this reason, ligands that do not display target selectivity, such as those reported in this study, should not be discarded a priori. We are currently investigating whether these compounds selectively inhibit parasite growth and interact with parasite telomeres in *P. falciparum* blood cultures.

Experimental Section

Oligonucleotides and compounds: All oligonucleotides and their fluorescent conjugates were purchased from Eurogentec (Seraing, Belgium), dissolved in doubly distilled water (at a concentration of about 300 μM), stored at −20 °C and used without further purification. Concentrations were determined by UV absorption with use of extinction coefficients determined from the nearest-neighbour model.[50]

The cationic porphyrin TMPyP4 (counterion $pCH_3(C_6H_4)SO_3^-$) and the perylene derivative PIPER were purchased from Calbiochem. The trisubstituted acridine BRACO-19 and the ethidium derivative 317050 (WO 0212194) were a kind gift from P. Mailliet (Sanofi–Aventis). Telomestatin was a kind gift from K. Shin-ya (University of Tokyo). The syntheses of bisquinolinium derivatives (Phen-DC3, Phen-DC6, Bipy-DC3 and Bipy-DC6 with counterion $CF_3SO_3^-$), neomycin-capped macrocycles (NCA1, NCA2, NCQ and NCphen), copper(II) terpyridine Cu-ttpy and metaquinacridines (MMQ1, MMQ3 and MMQ10) were described previously.[27–31] Telomestatin was dissolved (at 1 mM concentration) in DMSO/MeOH (1:1). TMPyP4 and the neomycin-capped derivatives were dissolved (at 2 mM and 1 mM, respectively) in doubly distilled water. PIPER was dissolved (2 mM) in acetic acid (10%). All the other compounds were dissolved at 2 mM in DMSO; all compounds were stored at −20 °C. Further dilutions were made in doubly distilled water.

***P. falciparum* cultures and parasite preparations**: *P. falciparum* (FCB1 strain) was maintained in vitro in human erythrocytes in RPMI 1640 medium supplemented by heat-inactivated human serum (8%, *v/v*) at 37 °C under CO_2 (3%), O_2 (6%) and N_2 (91%).[51] Synchronized cultures were obtained by a sequential combination of the gelatin flotation method[52] and sorbitol treatment.[53] Briefly, mature schizont-infected red blood cells were isolated and concentrated (to 60–80% parasitaemia) by use of Plasmion® (Fresenius Kabi). The schizonts were then put back in culture and diluted with fresh erythrocytes (to 10% parasitaemia). After 6 h, the reinvasion was stopped by lysis of the remaining schizont with sorbitol (5%, *w/v*, in doubly distilled water). Such a procedure yields parasite cultures synchronised in a 6 h window. For DNA preparation, infected red blood cells were washed twice in cold PBS and incubated for 5 min, on ice, in cold saponine in PBS (0.2%, *w/v*) in order to lyse the infected erythrocyte membrane without disrupting the parasite plasma membrane. Free parasites were then washed three times in cold PBS and stored at −80 °C until use.

***P. falciparum* genomic DNA extraction and exonuclease treatments**: Parasites (10^8, from erythrocytic cultures of the FCB1 strain) were diluted (100 μL in 1 mL, 10 vol) in an extraction solution containing Tris-HCl (10 mM, pH 8), EDTA (100 mM), SDS (0.5%) and RNase A (20 μg mL^{-1}; Sigma). Before use, RNase A was heated at 95 °C for 15 min to inactivate DNases. After being stirred for 1 h at 37 °C, an additional quantity of RNase A (20 μg mL^{-1}) was added, and digestion was continued for 1 h at 37 °C. Proteins and RNase A were then digested with proteinase K (100 μg mL^{-1}; Invitrogen) for 2.5 h at 50 °C. DNA was purified by phenol/chloroform extraction and precipitated by addition of ammonium acetate (0.2 vol, 7.5 M) and absolute ethanol (2.5 vol). The pellet was washed with ethanol (70%), air-dried and dissolved in TE buffer overnight at 4 °C. After determination of the DNA concentration by UV absorbance at 260 nm, aliquots of the genomic DNA solution were stored at −20 °C.

T7 Exonuclease (7.5 units, NEB) digestion of genomic DNA (4.5 μg) was carried out for 90 s at 25 °C in Tris acetate (20 mM, pH 7.9), potassium acetate (50 mM), magnesium acetate (10 mM) and dithiothreitol (1 mM; total volume: 50 μL). Exonuclease I (30 units, NEB) digestion of genomic DNA (4.5 μg) was carried out for 30 min at 37 °C in glycine/KOH (67 mM, pH 9.5), $MgCl_2$ (6.7 mM) and β-mercaptoethanol (10 mM; total volume: 50 μL). The reactions were stopped by addition of EDTA (25 mM). The exonuclease-treated DNA samples were precipitated with ethanol, dissolved in doubly distilled water (10 μL) and incubated for 30 min at 37 °C before use for the T-OLA.

Hybridisation assay with undigested DNA: The C-probe (d-(TGAACCC)$_3$) and G-probe (d(GGGTTTA)$_3$) (20 pmol) were 5′-radiolabelled with [γ^{32}P]ATP (80 μCi) and T4 polynucleotide kinase (10 units, NEB) in a T4 polynucleotide kinase reaction buffer (NEB) for 40 min at 37 °C (total volume: 30 μL) and purified on a Spin 6 column (Bio-Rad). The choice of probes bearing only three telomeric repeats was made to avoid folding of the G-probe into an intramolecular G-quadruplex; such folding could impair hybridisation to the target DNA. The C- and G-probe sequences were designed in order to minimise destabilisation upon hybridisation to the degenerate sequence of *Plasmodium* telomeres (a G–T mismatch should be less destabilising than an A–C mismatch).

Genomic DNA (3 μg) was incubated, overnight, at 37 °C or 50 °C with radiolabelled G- or C-probe (0.6 pmol) in Tris-HCl (10 mM, pH 7.9), NaCl (50 mM), $MgCl_2$ (10 mM) and dithiothreitol (1 mM; total volume: 20 μL). The samples were then loaded on a agarose gel (0.8%) in TBE buffer (1×) containing ethidium bromide. After migration in TBE buffer (1×), ethidium-stained DNA was analysed by UV transillumination at 254 nm. The gel was then vacuum-dried and exposed to a Phosphorimager screen, and scanned with a Typhoon 9410 instrument (GE Healthcare).

TRF assays: Telomere restriction fragment (TRF) assay was carried out as previously reported,[19] with minor modifications. Briefly, genomic DNA (3 μg) was digested, overnight, at 37 °C with a cocktail of four restriction enzymes (5 units of each): AluI, RsaI, DdeI and MboII (NEB). The reaction was carried out in Tris-HCl (10 mM, pH 7.9), NaCl (50 mM), $MgCl_2$ (10 mM) and dithiothreitol (1 mM; total volume: 30 μL). For the denaturing TRF assay, the digested sample was loaded on an agarose gel (0.8%) in TBE buffer (1×). After electrophoresis in TBE buffer (1×), analysis was performed by Southern blotting with the radiolabelled C-probe by using standard protocols. In a native TRF assay, the radiolabelled G- or C-probe (0.6 pmol) was added during the overnight digestion at 37 °C. The samples were then loaded on an agarose gel (0.8%) in TBE buffer (1×) containing ethidium bromide. After migration in TBE buffer (1×), ethidium fluorescence and radioactivity were imaged as described above. Radiolabelled and unlabelled 1 kb plus DNA ladders (Invitrogen) were loaded on the gels as size markers for radioactive and ethidium fluorescence detection, respectively.

T-OLA: Telomeric–oligonucleotide ligation assay (T-OLA) was carried out as previously described.[40] The C-probe (20 pmol) was 5′ radiolabelled with [γ^{32}P]ATP (80 μCi) and T4 polynucleotde kinase (10 units, NEB) in a T4 polynucleotide kinase reaction buffer (NEB) for 40 min at 37 °C (total volume: 20 μL). To ensure complete phosphorylation, an additional phosphorylation step was then carried out by addition of ATP (1 μL 0.1 M) and T4 polynucleotide kinase (1 μL, 10 U μL^{-1}, NEB) for 10 min at 37 °C. The radiolabelled probe was purified on a Spin 6 column (Bio-Rad).

Genomic DNA (3 μg) either treated or untreated with exonuclease I or T7 exonuclease was incubated, overnight, at 50 °C with the radiolabelled probe (0.6 pmol) in Tris-HCl (20 mM, pH 7.6), potassium acetate (25 mM), magnesium acetate (10 mM), dithiothreitol (10 mM), nicotinamide adenine dinucleotide (1 mM) and Triton X-100 (0.1%; total volume: 20 μL). The hybridisation step was followed by a ligation step (5 h) at 50 °C in the presence of Taq DNA ligase (20 units, NEB). Samples were then precipitated by addition of NaCl (80 μL, 0.625 M) and absolute ethanol (200 μL) and centrifuged for 15 min at 14000 *g*. Pellets were washed once with ethanol (70%), air-dried and incubated in doubly distilled water (10 μL) for 30 min at 50 °C. Samples (2 μL) were loaded on an agarose gel (0.8%) in TBE buffer (0.5×) containing ethidium bromide. After migration, ethidium fluorescence and radioactivity were imaged as described above. The ligated probes (7 μL of samples) were separated in a denaturing polyacrylamide gel (acrylamide/bisacrylamide 19:1 5%, in TBE 1× and urea 7 M).

UV measurements: UV absorbance spectra and melting curves were acquired by using a Kontron Uvikon 940 spectrophotometer. In the UV melting experiments the temperature was varied with a circulating water bath from 90 °C to 2 °C and from 2 °C to 90 °C at a rate of 0.2 °C min^{-1}. Evaporation at high temperatures was reduced by a layer of mineral oil, and condensation at low temperatures was minimised by use of a dry air flow in the sample compartment. Thermal difference spectra (TDS) were obtained by subtracting the absorbance spectrum at 2 °C from the one at 90 °C; the spectrum at 2 °C was recorded after annealing of the sample from 90 to 2 °C at a rate of 0.2 °C min^{-1}.

CD spectra were recorded by using a Jasco J-810 spectropolarimeter at 20 °C, after annealing from 90 °C at a rate of 1 °C min^{-1}. Two spectra were accumulated at a scan speed of 200 nm min^{-1}, and the contributions of the buffer and quartz cell were subtracted.

All experiments (melting, TDS and CD) were carried out at 3 μM or 30 μM oligonucleotide concentration in a cacodylic acid buffer (10 mM, pH 7.2, adjusted with LiOH) containing KCl or NaCl or LiCl (100 mM), in 1 cm or 0.2 cm pathlength cells.

FRET melting experiments: FRET melting experiments were carried out as described previously[47,54] with double-labelled oligonucleotides: the *Plasmodium* sequences FPf1T (FAM-$^{5'}$(GGGTTTA)$_3$-GGG$^{3'}$-TAMRA] and FPf8T (FAM-$^{5'}$(GGGTTCA)$_3$GGG$^{3'}$-TAMRA) and the human sequence F21GT (FAM-$^{5'}$(GGGTTA)$_3$GGG$^{3'}$-TAMRA). The FAM emissions at 516 nm of double-labelled telomeric sequences in the absence and presence of a single compound were recorded as a function of temperature by using a Stratagene MX3000P thermal block in 96-well microplates. To investigate the quadruplex versus duplex selectivity of each compound, a 26-base self-complementary competitor (ds26, $^{5'}$CAATCGGATCGAATTCGATCCGATTG$^{3'}$) was added. The temperature was varied from 25 °C to 95 °C (the temperature range of the MX3000P thermal block) at a rate of 1 °C min^{-1}. The FAM emission versus temperature plots were normalised between 0 and 1, and the temperature of half-dissociation ($T_{1/2}$) that corresponded to an emission value of 0.5 was determined.[47] The (quasi)complete folding of the labelled telomeric sequences at 25 °C, under our experimental conditions, was verified by performing FRET melting experiments between 0 °C and 80 °C on a SPEX Fluorolog (data not shown). All the experiments were carried out in duplicate with oligonucleotide (0.2 μM), compound (1 μM) and increasing concentrations of ds26 (0, 3 and 10 μM), in a cacodylic acid buffer (10 mM, pH 7.2, adjusted with LiOH) containing NaCl (100 mM) or KCl (10 mM) + LiCl (90 mM) in a total volume of 25 μL. For each compound, two or three independent experiments were performed.

Acknowledgements

We thank Anh Tuan Phan (Nanyang Technological University, Singapore), Patrick Mailliet and Eliane Mandine (Sanofi–Aventis, Vitry, France), Kazuo Shin-ya (University of Tokyo), Elsa De Lemos, Markus Kaiser and Candide Hounsou (Institut Curie, Orsay), and Jean-François Riou, Julien Gros, Aurore Guédin and Samir Amrane (Museum, Paris) for helpful discussions. This work was supported in part by an EU FP6 "MolCancerMed" grant (LSHC-CT-2004-502943 to J.-L.M.), the DGA (Program "Stress and transcrip-

tome of P. falciparum*") and the National Museum of Natural History (BQR 2007-2008).*

Keywords: DNA recognition · DNA structures · oligonucleotides · *Plasmodium* telomeres · quadruplexes

[1] R. J. Wellinger, D. Sen, *Eur. J. Cancer* **1997**, *33*, 735.
[2] M. T. Teixeira, E. Gilson, *Chromosome Res.* **2005**, *13*, 535.
[3] L. A. Klobutcher, M. T. Swanton, P. Donini, D. M. Prescott, *Proc. Natl. Acad. Sci. USA* **1981**, *78*, 3015.
[4] N. K. Jacob, R. Skopp, C. M. Price, *EMBO J.* **2001**, *20*, 4299.
[5] V. L. Makarov, Y. Hirose, J. P. Langmore, *Cell* **1997**, *88*, 657.
[6] R. McElligott, R. J. Wellinger, *EMBO J.* **1997**, *16*, 3705.
[7] W. E. Wright, V. M. Tesmer, K. E. Huffman, S. D. Levene, J. W. Shay, *Genes Dev.* **1997**, *11*, 2801.
[8] R. J. Wellinger, A. J. Wolf, V. A. Zakian, *Cell* **1993**, *72*, 51.
[9] K. Riha, T. D. McKnight, J. Fajkus, B. Vyskot, D. E. Shippen, *Plant J.* **2000**, *23*, 633.
[10] E. R. Henderson, E. H. Blackburn, *Mol. Cell. Biol.* **1989**, *9*, 345.
[11] C. W. Greider, E. H. Blackburn, *Cell* **1987**, *51*, 887.
[12] J. D. Griffith, L. Comeau, S. Rosenfield, R. M. Stansel, A. Bianchi, H. Moss, T. de Lange, *Cell* **1999**, *97*, 503.
[13] A. T. Phan, J. L. Mergny, *Nucleic Acids Res.* **2002**, *30*, 4618.
[14] A. M. Zahler, J. R. Williamson, T. R. Cech, D. M. Prescott, *Nature* **1991**, *350*, 718.
[15] D. Sun, B. Thompson, B. E. Cathers, M. Salazar, S. M. Kerwin, J. O. Trent, T. C. Jenkins, S. Neidle, L. H. Hurley, *J. Med. Chem.* **1997**, *40*, 2113.
[16] A. De Cian, L. Lacroix, C. Douarre, N. Temime-Smaali, C. Trentesaux, J. F. Riou, J. L. Mergny, *Biochimie* **2008**, *90*, 131.
[17] R. G. Ridley, *Nature* **2002**, *415*, 686.
[18] M. J. Gardner, N. Hall, E. Fung, O. White, M. Berriman, R. W. Hyman, J. M. Carlton, A. Pain, K. E. Nelson, S. Bowman, I. T. Paulsen, K. James, J. A. Eisen, K. Rutherford, S. L. Salzberg, A. Craig, S. Kyes, M. S. Chan, V. Nene, S. J. Shallom, B. Suh, J. Peterson, S. Angiuoli, M. Pertea, J. Allen, J. Selengut, D. Haft, M. W. Mather, A. B. Vaidya, D. M. Martin, A. H. Fairlamb, M. J. Fraunholz, D. S. Roos, S. A. Ralph, G. I. McFadden, L. M. Cummings, G. M. Subramanian, C. Mungall, J. C. Venter, D. J. Carucci, S. L. Hoffman, C. Newbold, R. W. Davis, C. M. Fraser, B. Barrell, *Nature* **2002**, *419*, 498.
[19] L. M. Figueiredo, L. H. Freitas-Junior, E. Bottius, J. C. Olivo-Marin, A. Scherf, *EMBO J.* **2002**, *21*, 815.
[20] E. Bottius, N. Bakhsis, A. Scherf, *Mol. Cell. Biol.* **1998**, *18*, 919.
[21] E. Dore, T. Pace, M. Ponzi, R. Scotti, C. Frontali, *Mol. Biochem. Parasitol.* **1986**, *21*, 121.
[22] M. T. Duraisingh, T. S. Voss, A. J. Marty, M. F. Duffy, R. T. Good, J. K. Thompson, L. H. Freitas-Junior, A. Scherf, B. S. Crabb, A. F. Cowman, *Cell* **2005**, *121*, 13.
[23] L. H. Freitas-Junior, R. Hernandez-Rivas, S. A. Ralph, D. Montiel-Condado, O. K. Ruvalcaba-Salazar, A. P. Rojas-Meza, L. Mancio-Silva, R. J. Leal-Silvestre, A. M. Gontijo, S. Shorte, A. Scherf, *Cell* **2005**, *121*, 25.
[24] D. K. Raj, B. R. Das, A. P. Dash, P. C. Supakar, *Biochem. Biophys. Res. Commun.* **2003**, *309*, 685.
[25] L. M. Figueiredo, E. P. Rocha, L. Mancio-Silva, C. Prevost, D. Hernandez-Verdun, A. Scherf, *Nucleic Acids Res.* **2005**, *33*, 1111.
[26] K. Chakrabarti, M. Pearson, L. Grate, T. Sterne-Weiler, J. Deans, J. P. Donohue, M. Ares, Jr., *RNA* **2007**, *13*, 1923.
[27] J. L. Mergny, L. Lacroix, M. P. Teulade-Fichou, C. Hounsou, L. Guittat, M. Hoarau, P. B. Arimondo, J. P. Vigneron, J. M. Lehn, J. F. Riou, T. Garestier, C. Hélène, *Proc. Natl. Acad. Sci. USA* **2001**, *98*, 3062.
[28] C. Hounsou, L. Guittat, D. Monchaud, M. Jourdan, N. Saettel, J. L. Mergny, M. P. Teulade-Fichou, *ChemMedChem* **2007**, *2*, 655.
[29] M. Kaiser, A. De Cian, M. Sainlos, C. Renner, J. L. Mergny, M. P. Teulade-Fichou, *Org. Biomol. Chem.* **2006**, *4*, 1049.
[30] A. De Cian, E. DeLemos, J.-L. Mergny, M.-P. Teulade-Fichou, D. Monchaud, *J. Am. Chem. Soc.* **2007**, *129*, 1856.
[31] H. Bertrand, D. Monchaud, A. De Cian, R. Guillot, J. L. Mergny, M. P. Teulade-Fichou, *Org. Biomol. Chem.* **2007**, *5*, 2555.
[32] F. Koeppel, J. F. Riou, A. Laoui, P. Mailliet, P. B. Arimondo, D. Labit, O. Petitgenet, C. Hélène, J. L. Mergny, *Nucleic Acids Res.* **2001**, *29*, 1087.
[33] F. Rosu, E. De Pauw, L. Guittat, P. Alberti, L. Lacroix, P. Mailliet, J. F. Riou, J. L. Mergny, *Biochemistry* **2003**, *42*, 10361.
[34] R. T. Wheelhouse, D. Sun, H. Han, F. X. Han, L. H. Hurley, *J. Am. Chem. Soc.* **1998**, *120*, 3261.
[35] O. Y. Fedoroff, M. Salazar, H. Han, V. V. Chemeris, S. M. Kerwin, L. H. Hurley, *Biochemistry* **1998**, *37*, 12367.
[36] M. Read, R. Harrison, B. Romagnoli, F. Tanious, S. Gowan, A. Reszka, W. Wilson, L. Kelland, S. Neidle, *Proc. Natl. Acad. Sci. USA* **2001**, *98*, 4844.
[37] S. M. Gowan, J. R. Harrison, L. Patterson, M. Valenti, M. A. Read, S. Neidle, L. R. Kelland, *Mol. Pharmacol.* **2002**, *61*, 1154.
[38] K. Shin-ya, K. Wierzba, K. Matsuo, T. Ohtani, Y. Yamada, K. Furihata, Y. Hayakawa, H. Seto, *J. Am. Chem. Soc.* **2001**, *123*, 1262.
[39] M. Y. Kim, H. Vankayalapati, K. Shin-Ya, K. Wierzba, L. H. Hurley, *J. Am. Chem. Soc.* **2002**, *124*, 2098.
[40] G. Cimino-Reale, E. Pascale, E. Battiloro, G. Starace, R. Verna, E. D'Ambrosio, *Nucleic Acids Res.* **2001**, *29*, e35.
[41] J.-L. Mergny, J. Li, L. Lacroix, S. Amrane, J. B. Chaires, *Nucleic Acids Res.* **2005**, *33*, e138.
[42] J. L. Mergny, A. T. Phan, L. Lacroix, *FEBS Lett.* **1998**, *435*, 74.
[43] Y. Wang, D. J. Patel, *Structure* **1993**, *1*, 263.
[44] A. Ambrus, D. Chen, J. Dai, T. Bialis, R. A. Jones, D. Yang, *Nucleic Acids Res.* **2006**, *34*, 2723.
[45] D. M. Gray, J. D. Wen, C. W. Gray, R. Repges, C. Repges, G. Raabe, J. Fleischhauer, *Chirality* **2008**, *20*, 431.
[46] J. L. Mergny, L. Lacroix, *Oligonucleotides* **2003**, *13*, 515.
[47] A. De Cian, L. Guittat, M. Kaiser, B. Sacca, S. Amrane, A. Bourdoncle, P. Alberti, M.-P. Teulade-Fichou, L. Lacroix, J.-L. Mergny, *Methods* **2007**, *42*, 183.
[48] P. Hazel, J. Huppert, S. Balasubramanian, S. Neidle, *J. Am. Chem. Soc.* **2004**, *126*, 16405.
[49] A. Guedin, A. De Cian, J. Gros, L. Lacroix, J. L. Mergny, *Biochimie* **2008**, *90*, 686.
[50] C. R. Cantor, M. M. Warshaw, H. Shapiro, *Biopolymers* **1970**, *9*, 1059.
[51] W. Trager, J. B. Jensen, *Science* **1976**, *193*, 673.
[52] J. B. Jensen, *Am. J. Trop. Med. Hyg.* **1978**, *27*, 1274.
[53] C. Lambros, J. P. Vanderberg, *J. Parasitol.* **1979**, *65*, 418.
[54] J. L. Mergny, J. C. Maurizot, *ChemBioChem* **2001**, *2*, 124.
[55] G. N. Parkinson, M. P. Lee, S. Neidle, *Nature* **2002**, *417*, 876.
[56] K. N. Luu, A. T. Phan, V. Kuryavyi, L. Lacroix, D. J. Patel, *J. Am. Chem. Soc.* **2006**, *128*, 9963.
[57] A. T. Phan, V. Kuryavyi, K. N. Luu, D. J. Patel, *Nucleic Acids Res.* **2007**, *35*, 6517.
[58] J. Dai, M. Carver, C. Punchihewa, R. A. Jones, D. Yang, *Nucleic Acids Res.* **2007**, *35*, 4927.

Received: May 14, 2008
Published online on October 16, 2008

